JOC Article

Generation and Characterization of the Selenocysteinyl Radical: Direct Evidence from Time-Resolved UV/Vis, Electron Paramagnetic Resonance, and Fourier Transform Infrared Spectroscopy

Christoph Kolano,*,† Götz Bucher,* Olaf Schade, Dirk Grote, and Wolfram Sander*

Lehrstuhl für Organische Chemie II der Ruhr-Universität Bochum, Universitätsstrasse 150, 44801 Bochum, Germany

wolfram.sander@rub.de; goetz.bucher@rub.de; c.kolano@pci.unizh.ch

Received March 10, 2005

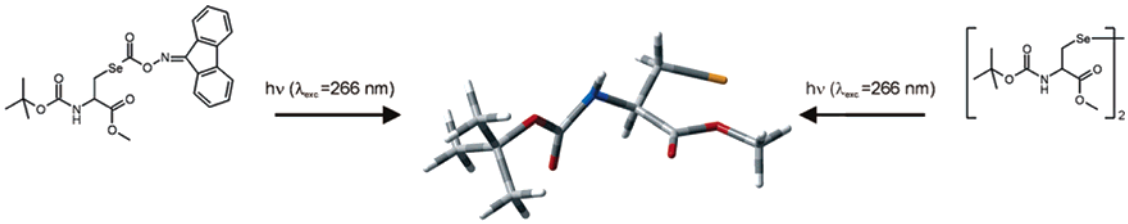

The selenocysteinyl radical **1** has been generated for the first time by laser flash photolysis (λ_{exc} = 266 nm) of dimethyl bis(N-*tert*-butoxycarbonyl)-L-selenocystine **2** and of [(9-fluorenylideneamino)-oxycarbonyl]methyl(N-*tert*-butoxycarbonyl)-L-selenocysteine **3** in acetonitrile and characterized by time-resolved (TR) UV/Vis, Fourier transform infrared (FTIR), and electron paramagnetic spectroscopy in combination with theoretical methods. A detailed product study was conducted using gas chromatography and one- and two-dimensional NMR spectroscopy. In the case of [(9-fluorenylideneamino)oxycarbonyl]methyl(N-*tert*-butoxycarbonyl)-L-selenocysteine **3**, the (9-fluorenylideneamino)oxycarbonyl moiety serves as a photolabile protection group providing a "caged selenocysteinyl radical" suitable for biophysical applications. Cleavage of the diselenide bridge or the selenium−carbonyl bond by irradiation is possible in high quantum yields. Because of the lack of a good IR chromophore in the mid-IR region, the selenocysteinyl radical **1** cannot be monitored directly by TR FTIR spectroscopy. TR UV/Vis spectroscopy revealed the formation of the selenocysteinyl radical **1** from both precursors. The selenocysteinyl radical **1** has a lifetime $\tau \approx 63$ μs and exhibits a strong band located at λ_{max} = 335 nm. Calculated UV absorptions of the selenocysteinyl radical (UB3LYP/6-311G(d,p)) are in good agreement with the experimental results. The use of TR UV/Vis spectroscopy permitted the determination of the decay rates of the selenocysteinyl radical in the presence of two quenchers. The product studies demonstrated the reversible photoreaction of dimethyl bis(N-*tert*-butoxycarbonyl)-L-selenocystine **2**. Products of the photolysis of the "caged selenocysteinyl radical" precursor **3** are dimethyl bis(N-*tert*-butoxycarbonyl)-L-selenocystine **2**, carbon dioxide, and some further smaller fragments. In addition, the photodecomposition of the (9-fluorenylideneamino)oxycarbonyl moiety produced 9-fluorenone-oxime **4**, 9-fluoren-imine **5**, and **6** and **7** as products of the dimerization of two 9-fluorenoneiminoxy radicals **8**.

Introduction

Selenium is a janus-faced element. While it is highly toxic, small doses of selenium are essential for the life of mammals and bacteria on earth. The toxicity is of relevance due to the use of selenium and selenium compounds in semiconductor and pharmaceutical industry as well as in synthetic organic chemistry.[1] As a trace element, on the other hand, it has found medical applications.[2,3] Thus, selenium shows strong interactions with heavy metals such as cadmium, silver, and mercury. Because of the significant concentrations of these heavy metals in marine food, supplements of selenium are required to diminish their toxic effects.

† Present address: Physikalisch-Chemisches Institut der Universität Zürich, Winterthurerstr. 190, CH-8057 Zürich, Switzerland.

(1) Ogawa, A. *Main Group Met. Org. Synth.* **2004**, *2*, 813−866.
(2) Liu, T. *Chem. Eng. News* **2003**, *81*, 94.
(3) Thomson, C. D. *Eur. J. Clin. Nutr.* **2004**, *58*, 391−402.

10.1021/jo050479j CCC: $30.25
Published on Web 07/20/2005

CHART 1. Established Selenyl Radicals

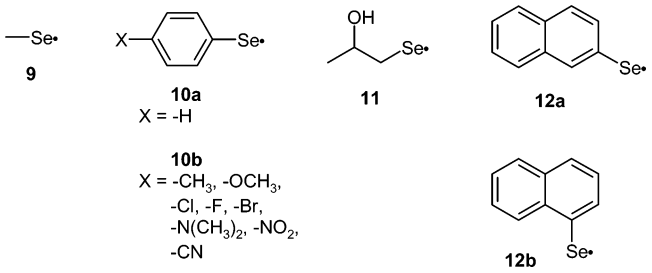

In biological systems, selenium occurs as a constituent of amino acids and other organic compounds, and in the last years the biological role of selenium amino acids has been intensely studied. Selenocysteine (Sec), selenocystine, and selenomethionine were found in the polypeptidic chains of several selenium-containing enzymes, among them glutathione peroxidase, selenoprotein P, glycine reductase, and thioredoxin reductase. Selenocysteine has been recognized as the 21st "natural" amino acid.[4] Among the selenoproteins, glutathione peroxidase is of major interest due to its ability to catalyze reduction of reactive oxygen species (ROS), namely, superoxide anion and hydroxyl radical, at expense of glutathione.[3,5−7]

It has been reported that selenium compounds (selenocystine and ebselen) are effective scavengers of highly reactive intermediates in the human body.[9] Thus, traces of these compounds are widely used as therapeutics to diminish the cytotoxic properties of the hydroxyl radical and the superoxide anion. Recently, the effect of selenium-containing therapeutics has been discussed controversially in the literature. There is strong evidence that, while selenium compounds may quench free radicals effectively, they are also involved in a mechanism that is responsible for a new secondary formation of this type of radicals.[7]

So far, organic selenium-centered radicals have not been much studied. Only five types of radicals have been investigated, none of them in context with a possible medical or biophysical application. Among them are the monomethyl selenide (**9**),[10] a series of para-substituted arylselenyl radicals **10a**−**b**,[11,12] the (2-hydroxyprop-1-yl) selenyl radical (**11**),[13] and the 1-naphthylselenyl and 2-naphthylselenyl radicals (**12a**−**b**)[14] (Chart 1).

Important properties of chalcogen-atom-centered radicals are their reactivity toward carbon−carbon multiple bonds and their high affinity toward heavy metals. Here we describe the generation and characterization of selenocysteinyl radical **1** using product studies (NMR spectroscopy and gas chromatography (GC)), time-resolved (TR) UV/Vis, Fourier transform infrared IR (FTIR), and electron paramagentic resonance (EPR), and theoretical methods giving detailed insights into the reactivity of a selenium centered radical of biological importance.

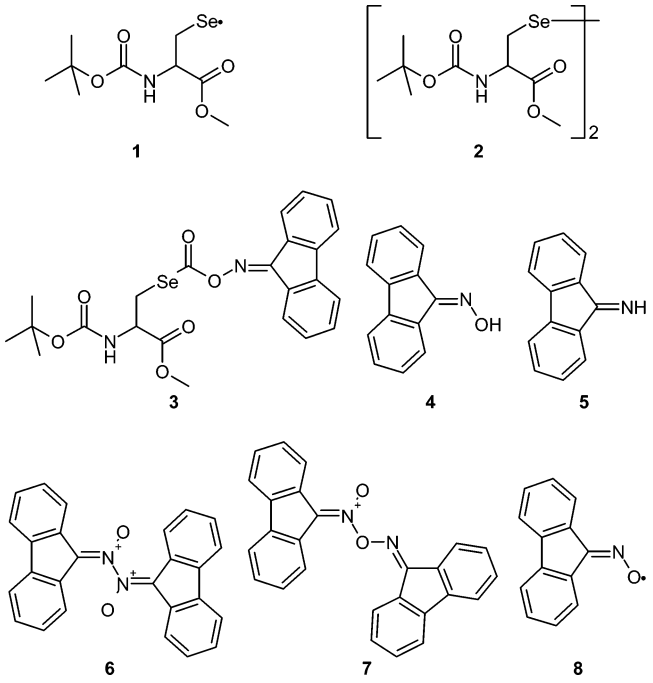

Results and Discussion

Dimethyl Bis(N-*tert*-butoxycarbonyl)-L-selenocystine 2. Laser flash photolysis (LFP) (λ_{exc} = 266 nm) of **2** in degassed CH_3CN led to the formation of a long-lived transient species with a first-order decay kinetics (k_{obs} = 1.6 × 10^4 s^{-1}, τ = 63 μs) and an absorption maximum λ_{max} = 335 nm. In addition, a short-lived transient species was observed with λ_{max} = 450 nm and a lifetime τ of 18 μs (k_{obs} = 5.4 × 10^4 s^{-1}) (Figures 1 and 2). None of the transients could be quenched by purging the solution with oxygen.

LFP studies had previously been carried out on naphthyl diselenides (1-NaphSe)$_2$ and (2-NaphSe)$_2$, which yielded the 1-naphthylselenyl and 2-naphthylselenyl radicals **12a**−**b** upon excitation.[14] These radicals exhibit absorption maxima at 420 and 680 nm for the 1-naphthylselenyl and 490 and 680 nm for the 2-naphthylselenyl radicals, respectively. Our results indicate that both the diselenide bridge (Se−Se cleavage, pathway (I)) and a C−Se bond (pathway (II)) are cleaved upon laser excitation of **2**, resulting in formation of the selenocysteinyl radical **1**, the diselenocysteinyl radical **13**, and the corresponding alkyl radical **14** (Scheme 1).

To confirm the assignment of the radical spectra, we calculated the UV/Vis spectra of the model radicals **15** and **16** (corresponding to **1** and **13** without the C- and N-terminal protecting groups) using time-dependent density functional theory (DFT) (TD-UB3LYP/6-311G(d,p)//UB3LYP/6-311G(d,p)). The calculated absorption maxima

(4) Anon *Eur. J. Biochem.* **1999**, *264*, 607−609.
(5) Stryer, L. *Biochemie*; 4. Auflage ed.; Heidelberg, Berlin, Oxford, 1996.
(6) Gettins, P.; Crews, B. C. *J. Biol. Chem.* **1991**, *266*, 4804−4809.
(7) Okuno, T.; Kawai, H.; Haegawa, T.; Ueno, H.; Nakamuro, K. *J. Health Sci.* **2001**, *47*, 240−247.
(8) Roussyn, I.; Briviba, K.; Masumoto, H.; Sies, H. *Arch. Biochem. Biophys.* **1996**, *330*, 216−218.
(9) Tappel, A. L.; Caldwell, K. A. *Science* **1967**, 345−361.
(10) BelBruno, J. J.; Spacek, J.; Christophy, E. *J. Phys. Chem.* **1991**, *95*, 6928−6932.
(11) Holm, A. H.; Yusta, L.; Carlqvist, P.; Brinck, T.; Daasbjerg, K. *J. Am. Chem. Soc.* **2003**, *125*, 2148−2157.
(12) Ito, O. *J. Am. Chem. Soc.* **1983**, *105*, 850−853.
(13) Barton, D. H. R.; Jacob, M.; Peralez, E. *Tetrahedron Lett.* **1999**, *40*, 9201−9204.
(14) Alam, M. M.; Ito, O.; Koga, Y.; Ouchi, A. *Int. J. Chem. Kinet.* **1998**, *30*, 193−200.

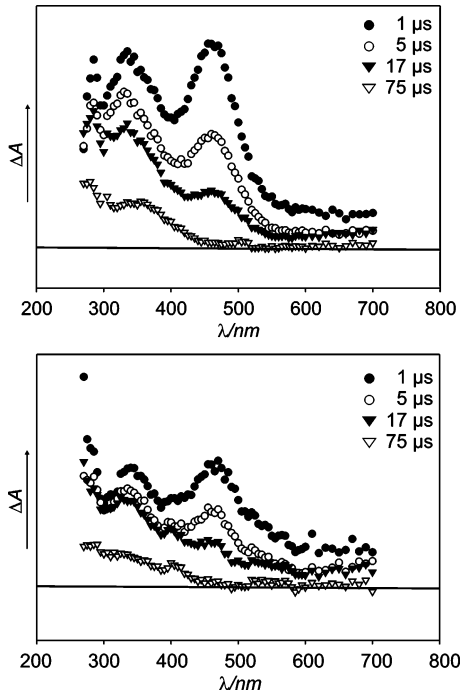

FIGURE 1. (Top) Transient absorption spectra following 266 nm laser excitation [traces recorded after 1 μs (black dots), 5 μs (white dots), 17 μs (black triangles), and 75 μs (white triangles), spectral resolution 5 nm, cell size 1.0 cm] in argon-purged acetonitrile displaying the photochemistry of **2**. (Bottom) Transient absorption spectra following 266 nm laser excitation [traces recorded after 1 μs (black dots), 5 μs (white dots), 17 μs (black triangles), and 75 μs (white triangles), spectral resolution 5 nm, cell size 1.0 cm] in oxygen-purged acetonitrile displaying the photochemistry of **2**.

SCHEME 1. Fragmentation Pattern of 2

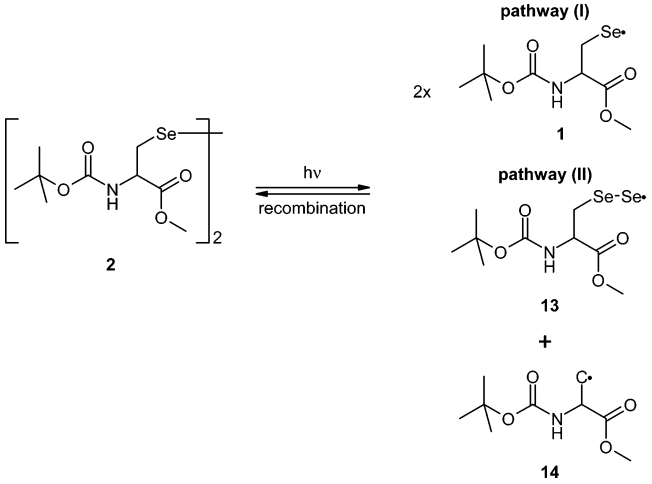

are in good agreement with the experimental results (Table 1).

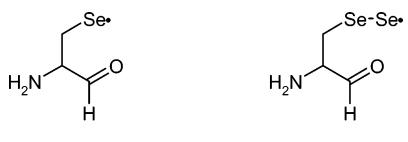

The phenylselenyl radical (**10a**) is known to react quickly with double and triple bonds in organic reactions.[15–17] Therefore, quenching experiments of **1** with tetramethylallene were performed (Figure 3). A rate constant of 1.1×10^5 L·mol^{-1}·s^{-1} was determined for this reaction.

In a similar way, the rate constant for the reaction of **1** with ethylpropiolate was determined to be 3.0×10^5 L·mol^{-1}·s^{-1} (Figure 4). The deviation from linearity of the regressions is caused by the absorption of laser light by the quencher at higher concentrations. The measurements have been performed in static cells where appropriate mixing of the solution is not guaranteed under all conditions. Thus, intramolecular reactions might influence the local concentrations of the quencher.

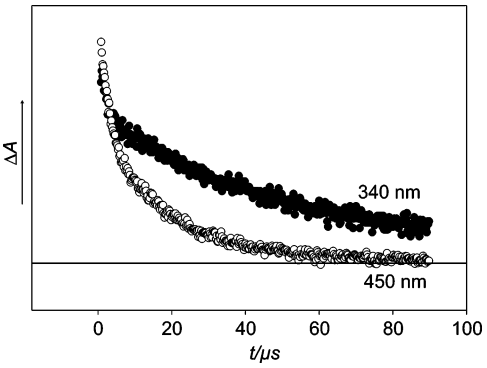

FIGURE 2. Transient decay traces, recorded at $\lambda = 340$ nm (black dots) and 450 nm (white dots), upon laser flash photolysis ($\lambda_{exc} = 266$ nm) of **2** in acetonitrile at ambient temperature.

TABLE 1. Observed and Calculated UV/Vis Maxima of the Selenocysteinyl Radical 15 and the Diselenocysteinyl Radical 16 as Models for the Protected Radicals 1 and 13

exptl λ (nm)	calcd λ (nm)[a] **15**	calcd rel int (%)[a] **15**	calcd λ (nm)[a] **16**	calcd rel int (%)[a] **16**
	648.8	6.1	501.5	61.2
450	490.6	100.0	464.3	65.7
335	363.2	8.1	399.5	100.0

[a] UB3LYP/6-311G(d,p).

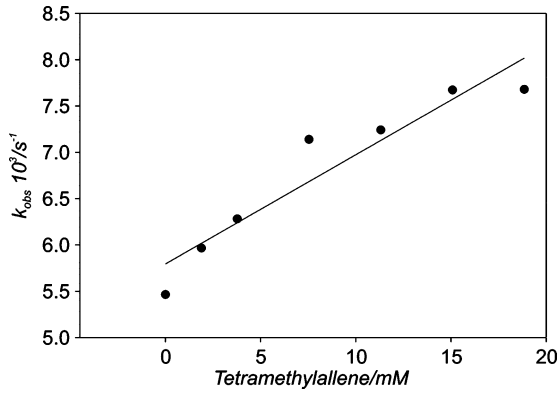

FIGURE 3. Decay rate of **1** in the presence of variable concentrations of tetramethylallene.

(15) Ogawa, A.; Doi, M.; Tsuchii, K.; Hirao, T. *Tetrahedron Lett.* **2001**, *42*, 2317–2319.
(16) Ogawa, A.; Yokoyama, K.; Yokoyama, H.; Sekiguchi, M.; Kambe, N.; Sonoda, N. *Tetrahedron Lett.* **1990**, *31*, 5931–5934.
(17) Ogawa, A.; Yokoyama, H.; Yokoyama, K.; Masawaki, T.; Kambe, N.; Sonoda, N. *J. Org. Chem.* **1991**, *56*, 5721–5723.

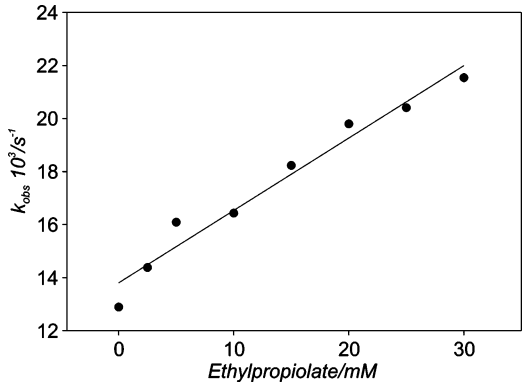

FIGURE 4. Decay rate of **1** in the presence of variable concentrations of ethylpropiolate.

These rate constants are in good agreement with the results obtained for the reaction of the phenyselenyl radical **10a** with allenes.[15−17] The reactivity of **1** is slightly higher than that of **10a**. This can be rationalized by some degree of stabilization of the phenylselenyl radical **10a** by the aromatic ring system.

Because of the lack of a good IR chromophore in the mid-IR region, the selenocysteinyl radical **1** cannot be monitored directly by TR FTIR. DFT calculations ((UB3LYP/6-311G(d,p)) on the model radicals **15** and **16** predict very weak stretching vibrations in the region around 630 cm^{-1} (δ_{C-Se} = 641.3 cm^{-1} of **15**, δ_{Se-Se} = 324.8 cm^{-1}, and δ_{C-Se} = 623.5 cm^{-1} of **16**), located in a spectral region not accessible to our TR FTIR spectrometer.

The formation of **1** as a major product of the photolysis of **2** was confirmed by product studies at ambient temperature. A degassed solution of **2** in CD_3CN was irradiated with the 266-nm light of a Nd:YAG laser. Before and after photolysis ^1H, ^{13}C, ^{77}Se, heteronuclear multiple quantum coherence (HMQC), and total correlation spectroscopy (TOCSY) NMR spectra were recorded. All signals in the spectra after irradiation can be clearly assigned to the starting material **2** (Table S3 and S4). Comparison of the ^{77}Se NMR spectra before and after irradiation ruled out the formation of other fragments or selenoorganic compounds (Figure S5). The apparent absence of photochemistry of **2** under conditions (laser irradiation) where fragmentation is observed in the LFP experiments indicates the efficient recombination of the fragment radicals **1** back to **2**. This recombination is obviously a quantitative reaction since no other products are formed.

[(9-Fluorenylideneamino)oxycarbonyl]methyl(N-*tert*-butoxy-carbonyl)-L-selenocysteine 3. It was recently shown that molecules functionalized with the (9-fluorenylideneamino)oxycarbonyl group are useful photo precursors for the generation of radicals.[18,19] Therefore, we synthesized [(9-fluorenylideneamino)oxycarbonyl]-methyl(N-*tert*-butoxycarbonyl)-L-selenocysteine **3** as an independent precursor for the selenocysteinyl radical **1**. Compound **3** should also be suitable as a "caged selenocysteinyl radical" in biophysical applications.

SCHEME 2. Syntheses of [(9-Fluorenylideneamino)oxycarbonyl]methyl(N-*tert*-butoxycarbonyl)-L-selenocysteine (3)

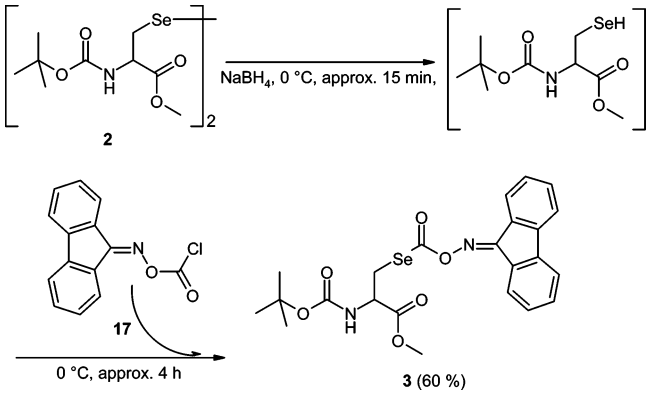

The synthesis of **3** is outlined in Scheme 2. The key intermediate, dimethyl bis(N-*tert*-butoxycarbonyl)-L-selenocystine **2**, was synthesized via a published procedure.[20−22] Reduction of the diselenide bridge of selenocystine **2** was achieved in the presence of sodium borohydride at low temperature, followed by the addition of 9-fluorenone-oxime-chloroformate **17**. [(9-Fluorenylideneamino)oxycarbonyl]methyl(N-*tert*-butoxycarbonyl)-L-selenocysteine **3** was obtained in good yields and shows excellent thermal stability.

LFP (λ_{exc} = 266 nm) of **3** in degassed CH_3CN at ambient temperature resulted in the bleaching of the 300 nm absorption, indicating dissociation of the precursor. A transient with λ_{max} = 660 nm and a lifetime of 4.2 μs was assigned to the 9-fluorenoneiminyl radical **18**, in agreement with published data.[23] In addition, a transient with λ_{max} = 340 nm overlapping with an absorption growing in was observed (Figure 5). Neither transient lifetimes nor absorption maxima were affected by purging the solution with oxygen.

A more detailed evaluation of the trace at 340 nm revealed a complex kinetic behavior (Figure 6). The transient initially decays with approximated first-order kinetics. At the same monitoring wavelength, a second-order growth (λ_{max} = 360 nm) partially overlapping with the decay is observed. A comparison between the initial part of the decay trace monitored at λ = 340 nm with the kinetic results obtained from the LFP of **2** revealed that both transients decay with the same kinetics (inset of Figure 6). Thus, the 340 nm transient (decay) is assigned to the selenocysteinyl radical **1**.

The assignment of the second-order growth proved to be more difficult, and structures **4**−**8**, **19**, and **20** were considered. 9-Fluorenoneoxime **4**, 9-fluorenoneketimine **5**, and 9-fluorenone **19** can be excluded on the basis of their known UV/Vis spectra (Table S1). Dimers of the 9-fluorenoneiminoxy radical **8** are another potential source of the transient growth observed. In an earlier study on the photochemistry of 9-fluorenone oxime carbamates, no spectroscopic evidence could be gained for

(18) Kolano, C.; Bucher, G.; Wenk, H. H.; Jager, M.; Schade, O.; Sander, W. *J. Phys. Org. Chem.* **2004**, *17*, 207−214.
(19) Bucher, G.; Halupka, M.; Kolano, C.; Schade, O.; Sander, W. *Eur. J. Org. Chem.* **2001**, 545−552.
(20) Barton, D. H. R.; Bridon, D.; Herve, Y.; Potier, P.; Thierry, J.; Zard, S. Z. *Tetrahedron* **1986**, *42*, 4983−4990.
(21) Hauge, S. *Acta Chem. Scand.* **1971**, *25*, 3081−3093.
(22) Gieselman, M. D.; Xie, L.; van der Donk, W. A. *Org. Lett.* **2001**, *3*, 1331−1334.
(23) Bucher, G.; Scaiano, J. C.; Sinta, R.; Barclay, G.; Cameron, J. *J. Am. Chem. Soc.* **1995**, *117*, 3848−3855.

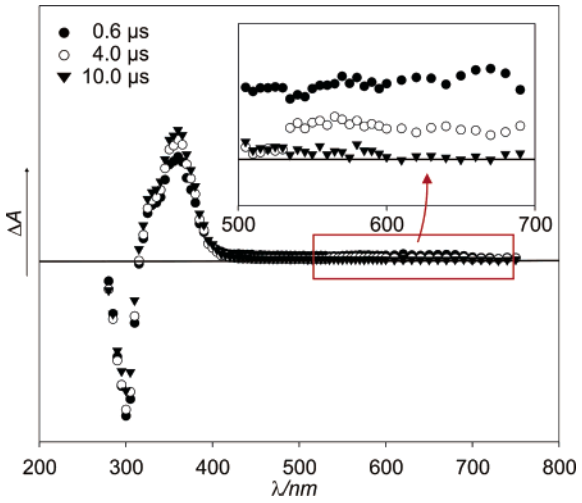

FIGURE 5. Transient absorption spectra following 266 nm laser excitation [traces recorded after 0.6 μs (black dots), 4 μs (white dots), and 10 μs (black triangles), spectral resolution 5 nm, cell size 1.0 cm] in argon-purged acetonitrile displaying the photochemistry of **3**. Inset: Magnification of the 500−700 nm region.

N−O cleavage competing with C−O scission, whereas product studies revealed the formation of fluorenone **19**.[23] The formation of **19** was explained by a dark reaction of fluorenoneimine **5** with water. However, further work has shown that hydrolysis of **5** cannot be the source of **19**, since no ^{18}O-labeled **19** was detected as product in the presence of $H_2{}^{18}O$ (Figure S7). It is therefore likely that iminoxy radical **8** is the precursor of **19**[24] and indeed plays a minor role in the photochemistry of derivatives of 9-fluorenone oxime.

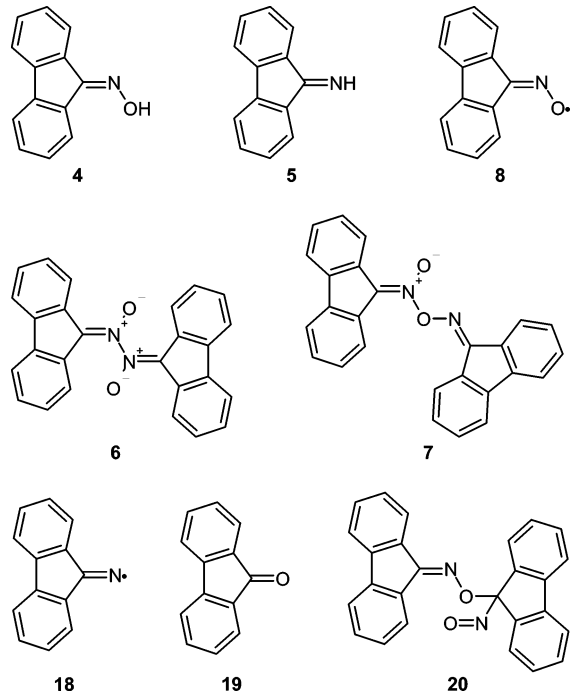

Ingold and co-workers earlier reported on the generation and characterization of stable dimers of iminoxy radicals derived from benzophenone oxime.[24] We calculated the UV/Vis spectra of the corresponding dimers **6**, **7**, and **20** using time-dependent DFT (TD-B3LYP/6-31+G*//B3LYP/6-31G*, Table S1). According to these calculations, **6** and **7** are two possible structures of the growing transient, since only these two compounds show strong absorptions between 340 and 360 nm necessary for the LFP detection. The transient growth at 340 nm is therefore tentatively assigned to the dimerization of **8** (which is not observed directly) yielding **6** or **7**.

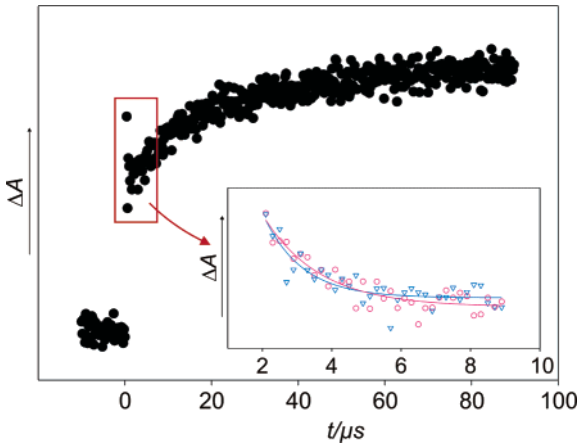

FIGURE 6. Transient decay trace, recorded at λ = 340 nm, upon LFP (λ_{exc} = 266 nm) of **3** in acetonitrile at ambient temperature. Inset: Comparison of the transient decay traces of **2** and **3**, recorded at λ = 340 nm (red dots, **2**; blue triangles, **3**), covering the time range up to 10 μs.

TR EPR and IR Experiments with 3. TR FTIR measurements were performed using the STEP/SCAN technique. LFP (λ_{exc} = 266 nm) with step-scan detection of **3** in acetonitrile (3.0 mM, argon purge) resulted in the bleaching of the 1743 cm^{-1} absorption of **3** and the concomitant formation of CO_2 ($\nu_{C=O_{as}}$ = 2342 cm^{-1}) (Figure 7). Within the time range of 20 μs covered by the experiments, no further transient signals were detected. A partial recovery of the signal after 20 μs indicates the formation of the starting material **3** (1728 cm^{-1}) and the stable photoproduct **2** (1746 cm^{-1}). Oxygen purging of the solution did also not lead to detectable transient signals.

LFP (λ_{exc} = 308 nm) of a 6.8 mM solution of **3** in CCl_4 (Ar purge) with TR EPR detection showed one transient set of signals, which evolves during the laser pulse. The 1:1:1 triplet centered at 3484 G (J_N = 9.52 G, g = 2.00331) reached maximum intensity after 220 ns and is assigned to the 9-fluorenoneiminyl radical **18** (Figure S8).[18,25]

The results from the STEP/SCAN and TR EPR measurements reveal that on irradiation **3** is cleaved into carbon dioxide, the selenocysteinyl radical **1**, and the 9-fluorenoneiminyl radical **18**. The fact that we were unable to detect the 9-fluorenoneiminoxy radical **8** by TR EPR (cf. g = 2.0064, α_N = 30.85, and α_H = 2.7)[26] indicates that formation of **8** is not a major photochemical pathway. This, however, does not rule out the formation of **8** in minor amounts as mentioned above.

(24) Brokenshire, J. L.; Roberts, J. R.; Ingold, K. U. *J. Am. Chem. Soc.* **1972**, *94*, 7040−7049.

(25) Forrester, A. R.; Gill, M.; Meyer, C. J.; Sadd, J. S.; Thomson, R. H. *J. Chem. Soc., Perkin Trans. 1* **1979**, 606−611.

(26) Gilbert, B. C.; Norman, R. O. C. *J. Chem. Soc. B* **1967**, 981−984.

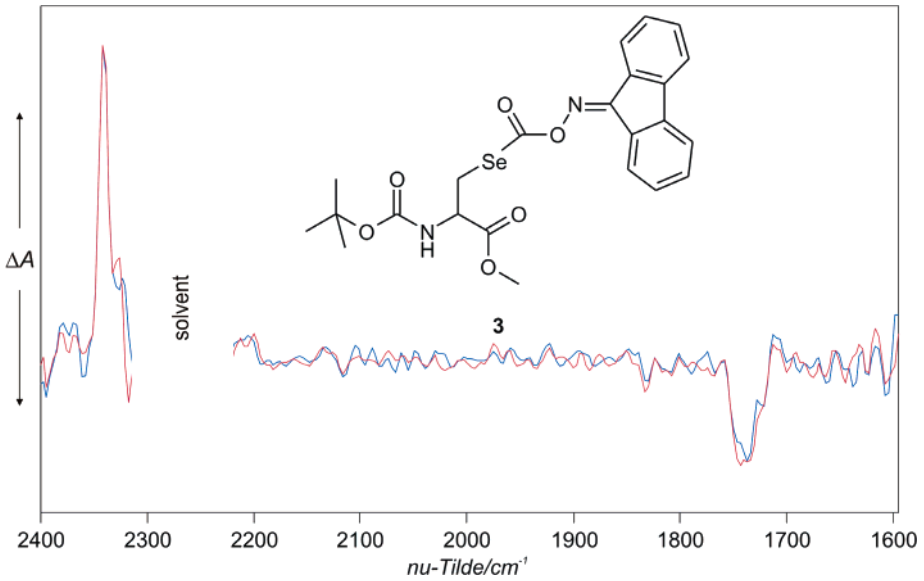

FIGURE 7. TR IR difference spectra (time resolution 500 ns, spectral resolution 6 cm^{-1}) showing the photochemistry of **3** in acetonitrile purged with argon. Bands appearing on irradiation (λ_{exc} = 266 nm) are pointing upward; bands disappearing are pointing downward. Red line, spectrum 500 ns after irradiation; blue line, spectrum after 20 μs.

Product Studies with 3. Product studies were carried out with **3** under the same conditions as described above for **2**. After irradiation of a CD_3CN solution of **3**, the ^1H and ^{13}C NMR spectra show a variety of new signals which could be assigned by using two-dimensional NMR spectroscopy (TOCSY, HMQC, and heteronuclear multiple-bond correlation (HMBC)). Major constituents were unreacted starting material **3** and dimethyl bis(*N*-*tert*-butoxycarbonyl)-L-selenocystine **2** (Table S2). In addition, carbon dioxide and compounds **4**−**7** were identified. This further confirms that iminoxy radical **8** is an intermediate in the photochemistry of **3**. ^{77}Se NMR spectroscopy is especially suitable to demonstrate the clean photochemistry of **3**. After irradiation of **3**, the ^{77}Se NMR spectrum shows one new signal of **2** approximately 100 ppm shifted toward high field. This reveals that **3** is converted directly into **2** via radical **1** without generating any other selenium containing molecules (Figure S6).

Conclusion

The selenocysteinyl radical **1** was generated from two independent precursors **2** and **3** and characterized by a variety of spectroscopic techniques and theoretical methods. On irradiation, selenocystine **2** undergoes reversible cleavage to produce the selenocysteinyl radical **1** as a short-lived radical pair. The lifetime of **1** produced from precursor **2** is limited by rapid thermal recombination of the radical pair. In precursor **3**, the C- and N-terminal protected selenocysteinyl radical is functionalized with the photolabile (9-fluorenylideneamino)oxycarbonyl group. Precursor **3** shows a high thermal stability and is readily cleaved by monochromatic 355 nm light. The photochemical cleavage of **3** is irreversible (in contrast to the cleavage of **2**) and leads to **1**, the 9-fluorenoneiminyl radical **18**, carbon dioxide, and small amounts of the 9-fluorenoneiminoxy radical **8**. Secondary products formed via thermal reactions of the primary radicals are **2**, 9-fluorenone-oxime **4**, and 9-fluoren-imine **5**. Although radical **8** could not be directly detected, the formation of its dimers **6** and **7** clearly indicate the presence of **8**. These results demonstrate that **3** is an excellent photochemical precursor of the selenocysteinyl radical **1** that could find broad applications in biophysical research as "caged selenocysteinyl".

Experimental Section

General Methods. Starting materials, reagents, and solvents were purchased from commercial suppliers and used without further purification. Solvents were dried by the usual methods. Na_2SO_4 was used as a drying agent unless otherwise reported. Chemical shifts (δ_H and δ_C) are reported in ppm with respect to internal solvent. δ_{Se} is expressed relative to a 50% (v/v) solution of Me_2Se in internal solvent. The abbreviations used are as follows: BOC, *tert*-butoxycarbonyl; MTBE, methyl tertiary-butyl ether; SeCys, selenocysteine; Ser, serine.

TR FTIR Spectroscopy (STEP/SCAN). For TR measurements, we used the STEP/SCAN setup that was described previously.[18,19,27] Excitation of the samples was carried out by the 4th harmonic (266 nm) of an Nd:YAG laser with a repetition rate of 10 Hz. To avoid thermal effects and shock waves, the laser energy was attenuated to 3.8−4.4 mJ/pulse by an external attenuator. All measurements were carried out with 6 cm^{-1} resolution in a spectral range between 0 and 3160 cm^{-1}, resulting in an interferogram containing 1060 points. The signal was averaged 20 times per sampling position. In all experiments, a time range of 20 μs was recorded with a resolution of 25 ns. After FT, the average of 20 successive spectra was calculated to achieve a better signal-to-noise ratio, resulting in an effective time resolution of 500 ns. The samples were dissolved (between 1.2 and 1.9 $g \cdot L^{-1}$, depending on the layer thickness of the cell) in acetonitrile (spectroscopic grade) and purged with argon for at least 45 min.

Nanosecond LFP. A standard LFP setup was used, consisting of a Nd:YAG laser, operated at 1 Hz and 266 nm (50 mJ/pulse, 8 ns pulse duration), a pulsed Xe arc lamp, a monochromator coupled to a photoelectron multiplier tube, and a digital oscilloscope. The entire setup was controlled from a personal computer using LabView software. Data evaluation was performed using SigmaPlot software. To avoid depletion of the precursor and product build up, a flow cell was used.

(27) Kolano, C.; Sander, W. *Eur. J. Org. Chem.* **2003**, 1074−1079.

Quenching experiments were performed in the same way, except that the flow cell was replaced by a static cell. The concentrations of **2** and **3** were adjusted so that an optical density of 0.3 was achieved at the laser wavelength used for excitation.

TR EPR. For TR EPR measurements, we used the setup described previously.[18] The concentration of **3** in tetrachloromethane was 6.83 mmol/L. The photoreaction was initiated by an excimer laser at $\lambda_{exc} = 308$ nm with a repetition rate of 10 Hz.

Product Studies. A product study was performed in the following manner: Samples of **2** and **3** (0.044 mol/L of **2** and 0.049 mol/L of **3**) were dissolved in [D3]acetonitrile, transferred in quartz NMR tubes, and degassed by the use of a supersonic bath and the "freeze and pump" technique. The tubes were fused, and ^{1}H, ^{13}C, ^{77}Se, TOCSY, HMQC, and HMBC NMR spectra were taken before and after the photolysis. Preparative photolysis was carried out with 0.42 W·s^{-1} for 1 h using a Nd:YAG laser operating at $\lambda_{exc} = 266$ nm with a repetition rate of 10 Hz. The irradiated NMR tubes were opened and the samples examined by analytical gas chromatography (OV 1 column, 10 m, $Ø_{inner}$ 0.1 mm).

Calculations. Calculations were performed with the Gaussian98 Rev.A11 suite of programs.[28] Stationary points, energies, and vibrational and UV spectra were calculated using the B3LYP[29] functional with a 6-311++g(d,p) or 6-31+g* basis set. The calculated vibrational frequencies given are unscaled.

Dimethyl Bis(N-*tert*-butoxycarbonyl)-L-selenocystine (2). Several protocols for the synthesis of **2** have been published in the literature.[20−22] Mp 94.0 °C. ^{1}H NMR (600.13 MHz, CD_3CN) δ 5.76 (d, 2H); 4.42 (m, 2H); 3.70 (s, 6H); 3.38 (m, 2H); 3.21 (m, 2H); 1.42 (s, 18H). ^{13}C NMR (150.9 MHz, CD_3CN) δ 172.4; 156.3; 80.4; 55.1; 53.0; 32.2; 28.5. ^{77}Se NMR (114.5 MHz, $CDCl_3$) δ 305.46. IR (KBr) cm^{-1} 3380, 2982, 2328, 1747, 1687, 1511, 1437, 1406, 1393, 1361, 1314, 1279, 1248, 1216, 1164, 1060, 1026, 1013, 980, 914, 856, 829, 781, 757, 652, 559, 386, 346, 203. Fast-atom bombardment mass spectroscopy (FAB-MS) in *m/z* (rel. %): 587.1 (54) $[M + Na]^+$, 562.1 (60) $[M + H]^+$, 507.1 (38), 408.9 (96), 146.0 (100), 57.1 (95). Anal. Calcd for $C_{18}H_{32}N_2O_8Se_2$ (562.38): C, 38.44; H, 5.74; N, 4.98; O, 22.76; Se, 28.08. Found: C, 38.95; H, 5.72; N, 4.93. These data agree with literature values.[22]

9-Fluorenone-oxime-chloroformate (17).[30,31] 9-Fluorenone-oxime (1.95 g, 0.01mol) was suspended in 200 mL of tetrachloromethane. A solution of phosgene in toluene (25 mL, $c = 2$ mol L^{-1}, 0.05 mol) was added dropwise at −7 °C. The suspension was stirred for 18 h. During that time, it was allowed to warm gradually to ambient temperature. Excess phosgene was then destroyed by purging the resulting solution with argon. The gaseous phosgene−argon mixture was led through a 20% aqueous sodium hydroxide solution for removal of the phosgene. After filtration of the organic solution, the solvent was removed and the yellow product was recrystallized from anhydrous *n*-hexane (ca. 1600 mL) yielding 2.32 g (90%) of pure **12**. Mp 132.0 °C (literature value[30] = 110−112 °C). ^{1}H NMR (200.13 MHz, $CDCl_3$) δ 8.17 (d, 1H); 7.85 (d, 1H); 7.60 (d, 1H); 7.58 (d, 1H); 7.51 (t, 1H); 7.46 (t, 1H); 7.35 (t, 1H); 7.30 (t, 1H). ^{13}C NMR (50.3 MHz, $CDCl_3$) δ 160.1; 148.1; 142.8; 141.5; 133.5; 132.5; 130.7; 129.4; 128.9; 128.6; 123.7; 120.5; 120.3. IR (KBr) cm^{-1} 3385, 1806, 1632, 1607, 1594, 1535, 1495, 1450, 1317, 1204, 1155, 1105, 1037, 964, 857, 784, 732, 666, 645. EI-MS *m/z* 257, 178, 164, 151, 76; UV λ_{max}/nm 214, 256, 300.

[(9-Fluorenylideneamino)oxycarbonyl]methyl(N-*tert*-butoxycarbonyl)-L-selenocysteine (3). In a flame-dried flask, dimethyl bis(*N*-*tert*-butoxycarbonyl)-L-selenocystine **2** (0.76 g, 1.33 mmol) was placed under Ar atmosphere. To this was added freshly distilled and dried acetonitrile (30 mL). $NaBH_4$ (0.14 g, 3.55 mmol) was added portionwise to the ice-cooled and vigorously stirred solution. Afterward the solution was stirred at room temperature until the color disappeared (approximately 15 min). The progress of the reduction can be checked by thin-layer chromatography (TLC). After that the reaction mixture was cooled again by an ice bath and a solution consisting of 0.904 g (3.55 mmol) **17** in 40 mL freshly distilled and dried acetonitrile was added dropwise. The solution was vigorously stirred for another 4 h under ice cooling, while the reaction was monitored by TLC. The solvent was evaporated and the pale-yellow residue was purified by column chromatography (hexane:MTBE 65:35). Yield: 0.805 g, (60.0%) of a pale-yellow solid. TLC (hexane:MTBE 65:35) R_f 0.32. Mp 148.0 °C. ^{1}H NMR (400.1 MHz, CD_3CN) δ 8.19 (d, 1H); 7.74 (m, 3H); 7.55 (m, 2H); 7.38 (m, 2H); 5.79 (d, 1H); 4.49 (m, 1H); 3.73 (s, 3H); 3.44 (m, 1H); 3.19 (m, 1H); 1.40 (s, 9H). ^{13}C NMR (100.6 MHz, CD_3CN) δ 172.5; 171.7; 158.2; 156.4; 143.6; 142.4; 134.6; 134.5; 133.4; 131.1; 130.3; 130.0; 129.7; 123.6; 121.8; 121.8; 80.4; 54.5; 53.1; 28.6; 28.5. ^{77}Se NMR (76.3 MHz, CD_3CN) δ 406.20; IR (KBr) cm^{-1} 3351, 2330, 1753, 1728, 1689, 1527, 1450, 1368, 1337, 1281, 1207, 1167, 1121, 1053, 950, 785, 733, 708, 643. FAB-MS in *m/z* (rel. %): 527.0 (78) $[M + Na]^+$, 505.1 (20) $[M + H]^+$, 196.0 (56), 154.0 (100), 136.0 (66). Anal. Calcd for $C_{29}H_{24}N_2O_6Se$ (503.42): C, 54.88; H, 4.81; N, 5.56; O, 19.07; Se, 15.68. Found: C, 54.72; H, 4.73; N, 5.36.

Acknowledgment. C.K. thanks the Deutsche Forschungsgemeinschaft for a Postdoctoral Research Fellowship. This work was financially supported by the Deutsche Forschungsgemeinschaft (SFB 452) and the Fonds der Chemischen Industrie. The authors thank Dr. F. Scheidt for valuable advice with the GC analysis and K. Gomann for his help with the TR EPR measurements of **2** and **3**.

Supporting Information Available: Instrumentation, calculated and experimental UV/Vis absorptions, ^{1}H and ^{13}C NMR data of the products of **3** after irradiation, GC data, 2D NMR spectra of **3**, ^{77}Se NMR spectra of **2** and **3** before and after irradiation, distribution of the products after photolysis, calculated energies, geometries and vibrational modes of **15** and **16**, optimized Cartesian coordinates for compounds arising from recombination of **8**, and TR EPR spectrum. This material is free of charge via the Internet at http://pubs.acs.org.

JO050479J

(28) Frisch, M. J.; Trucks, G. W.; Schlegel, H. B.; Scuseria, G. E.; Robb, M. A.; Cheeseman, J. R.; Zakrzewski, V. G.; Montgomery, J. A., Jr.; Stratmann, R. E.; Burant, J. C.; Dapprich, S.; Millam, J. M.; Daniels, A. D.; Kudin, K. N.; Strain, M. C.; Farkas, O.; Tomasi, J.; Barone, V.; Cossi, M.; Cammi, R.; Mennucci, B.; Pomelli, C.; Adamo, C.; Clifford, S.; Ochterski, J.; Petersson, G. A.; Ayala, P. Y.; Cui, Q.; Morokuma, K.; Salvador, P.; Dannenberg, J. J.; Malick, D. K.; Rabuck, A. D.; Raghavachari, K.; Foresman, J. B.; Cioslowski, J.; Ortiz, J. V.; Baboul, A. G.; Stefanov, B. B.; Liu, G.; Liashenko, A.; Piskorz, P.; Komaromi, I.; Gomperts, R.; Martin, R. L.; Fox, D. J.; Keith, T.; Al-Laham, M. A.; Peng, C. Y.; Nanayakkara, A.; Challacombe, M.; Gill, P. M. W.; Johnson, B.; Chen, W.; Wong, M. W.; Andres, J. L.; Gonzalez, C.; Head-Gordon, M.; Replogle, E. S.; Pople, J. A. *Gaussian98*, revision A.11.1; Gaussian, Inc.: Pittsburgh, PA, 2001.
(29) Becke, A. D. *J. Chem. Phys.* **1993**, *98*, 5648−5652.
(30) Beak, P.; Barron, J. A. *J. Org. Chem.* **1973**, *38*, 2771−2775.
(31) Jumar, A.; Held, P.; Schulze, W. *Z. Chem.* **1967**, *7*, 344−345.
(32) Gombler, W. *Z. Naturforsch. B* **1981**, *36B*, 1561−1565.